

TURBULENT BOUNDARY LAYER ON A FLAT PLATE IN AN  
INCOMPRESSIBLE FLUID

G.S.Glushko

FACILITY FORM 902	N66 24912	
	(ACCESSION NUMBER)	(THRU)
	29 (PAGES)	1 (CODE)
	(NASA CR OR TMX OR AD NUMBER)	12 (CATEGORY)

Translation of "Turbulentnyy pogranichnyy sloy na ploskoy  
plastine v neszhimayemoy zhidkosti".  
Izvestiya Akademii Nauk SSSR, Seriya Mekhanika,  
No.4, pp.13-23, 1965.

GPO PRICE \$ \_\_\_\_\_

CFSTI PRICE(S) \$ \_\_\_\_\_

Hard copy (HC) 2.00

Microfiche (MF) .50

# 653 July 65

NATIONAL AERONAUTICS AND SPACE ADMINISTRATION  
WASHINGTON APRIL 1966

TURBULENT BOUNDARY LAYER ON A FLAT PLATE IN AN  
INCOMPRESSIBLE FLUID

\*/13

G.S.Glushko

24912

Analysis showing that the effective viscosity created by Reynolds stresses during turbulent motion in the boundary layer is a function of the turbulent Reynolds number and only of the turbulent Reynolds number. This number comprises the total turbulent energy, the scale of turbulence, and molecular viscosity. This function is shown to be universal for turbulent boundary-layer flows and to be independent of the presence of a pressure gradient. An analytical relation between the effective viscosity and the turbulent Reynolds number is derived from processed measurements of the turbulence characteristics. With this relation, it is possible to use, instead of six equations for the second moments, only one equation for the total turbulent energy. A system of differential equations consisting of the Reynolds equation, the equation of total turbulent energy, an empirical distribution of the turbulence scale, and an empirical relation for the dissipation energy is integrated on an electronic digital computer. The solution obtained exhibits a laminar, a turbulent, and a transition region. The beginning of the transition region and the behavior of the solution in this region depend on the value

---

\* Numbers in the margin indicate pagination in the original foreign text.

of turbulent energy in the initial cross section. In the laminar and turbulent regions, the solution is independent of this value. The velocity distribution and distribution of total turbulent energy are obtained, and a relation between the friction coefficient and Reynolds number is derived. The results are compared with the experiment.

*Author*

It is shown in this paper that the effective viscosity, arising as a consequence of Reynolds stresses during turbulent motion in the boundary layer, is a function only of the "Reynolds turbulence number" composed of the total energy of turbulence, the scale of turbulence, and molecular viscosity. With the assumptions made here, this function is shown to be universal for turbulent flows of the boundary-layer type and does not depend on the presence of a pressure gradient. The specific type of dependence of the effective viscosity on the Reynolds turbulence number is obtained by analysis of the measurements of the turbulence characteristics.

The dependence found makes it possible to manage with one equation for the total energy of turbulence, in place of the six equations for second moments. For the third moments entering the equation of the total energy of turbulence and characterizing the spatial diffusion of the energy of turbulence, in this work, as in those of other authors, we introduce the "gradient concept" and assume that the diffusion coefficient is a function only of the Reynolds turbulence number. A comparative evaluation of the terms of the equation of total energy of turbulence for the case of flow in boundary layers shows that the terms containing the third moments are small in comparison with the principal terms. Therefore, the diffusion coefficient of the total energy of turbulence cannot be given exactly. Here, the dependence obtained from experiments on the

attenuation of homogeneous turbulence is used for the terms expressing the dissipation of energy.

The system of differential equations, consisting of Reynolds equations and the equation for the total energy of turbulence, which is supplemented by the empirical dependences mentioned above and by the empirical turbulence scale, was integrated on an electronic digital computer for the particular case of a flat plate.

It was found that three regions can be distinguished in the solution obtained: laminar, transitional, and turbulent. The start of the transitional region and the character of the behavior of the solution in this region depend on the value of the turbulent energy at the initial cross section. In the laminar and turbulent regions the solution does not depend on the value of the turbulent energy at the initial cross section. This paper gives the velocity distribution and the total turbulent energy distribution as well as the dependences of the friction coefficient on the Reynolds number; the results are compared with experimental data.

### Symbols

$\nu$  = kinematic viscosity

$\rho$  = density

$t$  = time

$U_i$  = components of the mean velocity vector ( $i, j, k = 1, 2, 3$ )

$P$  = mean pressure

$x_i$  = rectilinear rectangular coordinates ( $i = 1, 2, 3$ )

$\delta_{ij}$  = Kronecker delta

$u_i$  = components of the velocity fluctuation vector ( $i = 1, 2, 3$ )

$p$  = pressure fluctuation  
 $R$  = Reynolds number  
 $\delta$  = boundary-layer thickness  
 $l$  = characteristic length of flow surface  
 $U_\infty$  = velocity at edge of the boundary layer  
 $\epsilon$  = dimensionless "turbulent viscosity"  
 $u_\tau$  = dynamic velocity  
 $\tau_w$  = friction stress on flow surface  
 $C_f$  = friction coefficient of plate  
 $\eta$  = dimensionless coordinate

$$R = \frac{U_\infty l}{\nu}, \quad R_\delta = \frac{U_\infty \delta}{\nu}, \quad C_f = \frac{2}{\rho U_\infty^2 x_1} \int_0^{x_1} \tau_w(x_1) dx_1.$$

The  $x_1$  and  $x_3$  axes are directed parallel to the flow surface respectively along and across the mean flow; the  $x_2$  axis is perpendicular to the flow surface.

1. As is known [see, for example (Bibl.1)], the average values of the /14 quantities characterizing the flow (velocity vector components, pressure) in turbulent flows of an incompressible fluid obey the Reynolds equations:

$$\frac{\partial U_i}{\partial t} + \sum_{k=1}^3 U_k \frac{\partial U_i}{\partial x_k} = -\frac{1}{\rho} \frac{\partial P}{\partial x_i} + \nu \sum_{k=1}^3 \frac{\partial^2 U_i}{\partial x_k^2} - \sum_{k=1}^3 \frac{\partial \langle u_i u_k \rangle}{\partial x_k} \sum_{k=1}^3 \frac{\partial U_k}{\partial x_k} = 0. \quad (1.1)$$

Upper-case letters designate average values, and lower-case letters denote fluctuating values;  $\langle \rangle$  signifies averaging. By averaging, we mean time-averaging since stationary flows will be examined from now on.

From the Navier-Stokes equations we obtain, by well-known methods [see, for example (Bibl.2, 3)], the equations for the components of the tensor of turbulent stress entering eq.(1.1):

$$\begin{aligned}
& \frac{\partial \langle u_i u_j \rangle}{\partial t} + \sum_{k=1}^3 U_k \frac{\partial \langle u_i u_j \rangle}{\partial x_k} + \sum_{k=1}^3 \left( \langle u_k u_j \rangle \frac{\partial U_i}{\partial x_k} + \langle u_k u_i \rangle \frac{\partial U_j}{\partial x_k} \right) - \\
& - \frac{1}{\rho} \left\langle p \left( \frac{\partial u_i}{\partial x_j} + \frac{\partial u_j}{\partial x_i} \right) \right\rangle + 2\nu \sum_{k=1}^3 \left\langle \frac{\partial u_i}{\partial x_k} \frac{\partial u_j}{\partial x_k} \right\rangle + \\
& + \sum_{k=1}^3 \frac{\partial}{\partial x_k} \left[ -\nu \frac{\partial \langle u_i u_j \rangle}{\partial x_k} + \langle u_k u_i u_j \rangle + \frac{1}{\rho} \langle p (\delta_{ik} u_j + \delta_{jk} u_i) \rangle \right] = 0. \quad (1.2)
\end{aligned}$$

(i, j = 1, 2, 3)

The mechanical meaning of the individual terms in eqs.(1.2) can best be explained for  $i = j$ . In this case, the equations describe the behavior of the energy of fluctuations of an individual component of the velocity vector:

$$\begin{aligned}
& \frac{\partial \langle e_i \rangle}{\partial t} + \sum_{k=1}^3 U_k \frac{\partial \langle e_i \rangle}{\partial x_k} + \sum_{k=1}^3 \langle u_i u_k \rangle \frac{\partial U_i}{\partial x_k} - \frac{1}{\rho} \left\langle p \frac{\partial u_i}{\partial x_i} \right\rangle + \\
& + \sum_{k=1}^3 \frac{\partial}{\partial x_k} \left[ -\nu \frac{\partial \langle e_i \rangle}{\partial x_k} + \langle u_k e_i \rangle + \delta_{ik} \frac{1}{\rho} \langle p u_i \rangle \right] + \nu \sum_{k=1}^3 \left\langle \left( \frac{\partial u_i}{\partial x_k} \right)^2 \right\rangle = 0. \quad (1.3)
\end{aligned}$$

( $e_i = u_i^2/2$ ,  $i = 1, 2, 3$ )

The first two terms of eqs.(1.3) characterize the total time rate of change of the energy. The third term characterizes the work of Reynolds stresses, converting the energy of the mean flow to the fluctuation energy of a given velocity component. The fourth term characterizes the process of fluctuation energy transfer between the individual components of the velocity vector by means of pressure fluctuations. The fifth term characterizes the spatial diffusion of the fluctuation energy. Finally, the last term characterizes the dissipation of the fluctuation energy.

We will examine the problem of a stationary plane turbulent boundary layer. In this case, the partial derivatives from the average quantities with respect to time and the coordinate  $x_3$  will be equal to zero. The velocity vector component  $U_3$  will also be identically equal to zero. As a consequence of this,  $\langle u_1 u_3 \rangle$  and  $\langle u_2 u_3 \rangle$  do not enter into the equations for the remaining  $\langle u_i u_j \rangle$ .

Therefore, the equations for  $\langle u_1 u_3 \rangle$  and  $\langle u_2 u_3 \rangle$  will be discarded. In this case, they can also be determined from the experimental data from which it is known that, in a plane boundary layer,  $\langle u_1 u_3 \rangle = \langle u_2 u_3 \rangle = 0$ .

The terms are estimated in eqs.(1.1) and (1.2). The square root of the ratio of the boundary layer thickness to the characteristic length of the flow surface is taken as a smallness parameter. For a turbulent boundary layer on a flat plate, we have  $\delta/l = 0.37 R^{-0.2}$ . When  $R$  changes in the range from  $R = 10^5$  to  $R = 10^7$ , the ratio  $(\delta/l)^{1/2}$  changes from 20% to 12%, i.e., the quantity  $\frac{1}{15} (\delta/l)^{1/2}$  is approximately by one order smaller than unity. Therefore, in eqs.(1.1) and (1.2) we discard the terms starting with an order of smallness  $(\delta/l)^{1/2}$ . This leaves only terms of the order of unity.

We will assume that in the turbulent boundary layer the inertia forces, which are expressed by the left-hand side of eq.(1.1), are equal in order of magnitude to the forces of viscous and turbulent stresses. Furthermore, it is known from the experimental data that in the case under consideration all  $\langle u_i u_j \rangle$  are of the same order [except  $\langle u_1 u_3 \rangle$  and  $\langle u_2 u_3 \rangle$  which are equal to zero]. Hence, it follows that  $\langle u_i u_j \rangle \sim U_\infty^2 \delta/l$  and  $\nu \sim U_\infty^2 \delta/l$ . As a result, eqs.(1.1) take the usual form:

$$\begin{aligned} U_1 \frac{\partial U_1}{\partial x_1} + U_2 \frac{\partial U_1}{\partial x_2} &= -\frac{1}{\rho} \frac{\partial P}{\partial x_1} + \nu \frac{\partial^2 U_1}{\partial x_2^2} - \frac{\partial \langle u_1 u_2 \rangle}{\partial x_2} \\ \frac{\partial U_1}{\partial x_1} + \frac{\partial U_2}{\partial x_2} &= 0, \quad \frac{\partial P}{\partial x_2} = 0. \end{aligned} \quad (1.4)$$

It follows from an estimate of the terms in eqs.(1.2) that, in all equations, we can neglect terms expressing the total time rate of change and the diffusion of the tensor components of turbulent stresses. Among the terms expressing the work of Reynolds stresses, only the terms  $\langle u_1 u_2 \rangle \partial U_1 / \partial x_2$  [in the equation for  $\langle u_1^2 \rangle$ ] and  $\langle u_2^2 \rangle \partial U_1 / \partial x_2$  [in the equation for  $\langle u_1 u_2 \rangle$ ] are of the

order of unity. Since we are examining a stationary case so that the tensor components of the turbulent stresses do not increase in time, energy balance should exist at each point. Therefore, in the equations for  $\langle u_1^2 \rangle$  and  $\langle u_1 u_2 \rangle$  the terms expressing the dissipation of the turbulent stress tensor should also be of the order of unity. Since the dissipation occurs in small-scale fluctuations which are isotropic, the dissipative terms in other equations should also be of the order of unity. However, it is known from experimental data that  $\langle u_2^2 \rangle$  and  $\langle u_3^2 \rangle$  are of the same order as  $\langle u_1^2 \rangle$  and  $\langle u_1 u_2 \rangle$ . Consequently, the energy source should be of the order of unity, which would maintain  $\langle u_2^2 \rangle$  and  $\langle u_3^2 \rangle$  at such a level. The terms expressing energy transfer between components can be the only terms causing energy fluctuations of  $\langle u_2^2 \rangle$  and  $\langle u_3^2 \rangle$ , which can be of the order of unity. Consequently, the system of equations (1.2) takes the following form, in accordance with the above estimates and discussions:

$$\begin{aligned}
 \langle u_1 u_2 \rangle \frac{\partial U_1}{\partial x_2} - \frac{1}{\rho} \left\langle p \frac{\partial u_1}{\partial x_1} \right\rangle + \nu \sum_{k=1}^3 \left\langle \left( \frac{\partial u_1}{\partial x_k} \right)^2 \right\rangle &= 0 \\
 - \frac{1}{\rho} \left\langle p \frac{\partial u_2}{\partial x_2} \right\rangle + \nu \sum_{k=1}^3 \left\langle \left( \frac{\partial u_2}{\partial x_k} \right)^2 \right\rangle &= 0 \\
 - \frac{1}{\rho} \left\langle p \frac{\partial u_3}{\partial x_3} \right\rangle + \nu \sum_{k=1}^3 \left\langle \left( \frac{\partial u_3}{\partial x_k} \right)^2 \right\rangle &= 0 \\
 \langle u_2^2 \rangle \frac{\partial U_1}{\partial x_2} - \frac{1}{\rho} \left\langle p \left( \frac{\partial u_1}{\partial x_2} + \frac{\partial u_2}{\partial x_1} \right) \right\rangle + 2\nu \sum_{k=1}^3 \left\langle \frac{\partial u_1}{\partial x_k} \frac{\partial u_2}{\partial x_k} \right\rangle &= 0.
 \end{aligned} \tag{1.5}$$

2. Proceeding from the assumption that the portion of energy transferred by pressure fluctuations from  $\langle u_1^2 \rangle$  to  $\langle u_j^2 \rangle$  is proportional to their difference, Rotta (Bibl.2) obtained the following formula [see also (Bibl.3)]:

$$\frac{1}{\rho} \left\langle p \left( \frac{\partial u_i}{\partial x_i} + \frac{\partial u_j}{\partial x_j} \right) \right\rangle = K \frac{V \bar{e}}{L} \left( \langle u_i u_j \rangle - \frac{2}{3} \delta_{ij} e \right), \quad (2e = \langle u_1^2 \rangle + \langle u_2^2 \rangle + \langle u_3^2 \rangle). \tag{2.1}$$

Here  $L$  is the scale of turbulence,  $K$  is a certain constant, and  $e$  is the 16 energy of turbulence.



For terms expressing the dissipation of the components of the tensor of turbulent stresses, Rotta in the same work (Bibl.2) on the basis of experimental data proposed a formula similar to the following:

$$\nu \sum_{k=1}^3 \left\langle \frac{\partial u_i}{\partial x_k} \frac{\partial u_j}{\partial x_k} \right\rangle = \nu C \left( \frac{\langle u_i u_j \rangle}{2L^2} + \delta_{ij} \kappa \frac{\sqrt{\epsilon} L}{\nu} \frac{\epsilon}{3L^2} \right) \quad (2.2)$$

where  $C$  and  $\kappa$  are constants. Let us substitute eqs.(2.1) and (2.2) into the system (1.5); after easy calculations we obtain

$$\epsilon = - \frac{\langle u_1 u_2 \rangle}{\nu (\partial U_1 / \partial x_2)} = \frac{r^3}{(r + \beta)(r + \gamma)} \alpha r \quad (2.3)$$

$$\left( r = \frac{\sqrt{\epsilon} L}{\nu} \right).$$

Here,  $r$  is the Reynolds number of turbulence, while  $\alpha$ ,  $\beta$ ,  $\gamma$  are constants expressed by  $K$ ,  $C$ , and  $\kappa$ .

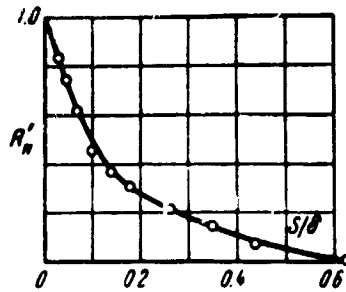


Fig.1

Thus, in a turbulent boundary layer the dimensionless "turbulent viscosity"  $\epsilon$  is a function only of the Reynolds number of turbulence. However, eqs.(2.1) and (2.2) were obtained under rather gross assumptions, so that eq.(2.3) indicates only the possibility of the existence of such a regularity and is in need of experimental confirmations.

3. To determine the dependence  $\epsilon(r)$  from the experimental data, we need measure all the quantities entering into the determination of  $\epsilon$  and  $r$  (i.e.,  $\langle u_1^2 \rangle$ ,  $\langle u_2^2 \rangle$ ,  $\langle u_3^2 \rangle$ ,  $\langle u_1 u_2 \rangle$ ,  $L$ ,  $\partial U_1 / \partial x_2$ ,  $\nu$ ) at each point of the turbulent boundary

layer or other turbulent flow in which the estimates which led to systems of equations (1.4) and (1.5) hold true (for example, a plane wake, a plane flow, a plane channel). Only in this case can we obtain the dependence  $\epsilon(r)$ . Unfortunately, there are very few works in the literature in which all of the above quantities have been measured. In most works, only some of these quantities have been measured. A number of papers give data on the measurements of some group of characteristics of turbulence without an accurate description of the experimental conditions [for example, the distribution of  $\langle u_1 u_1 \rangle / U_\infty^2$  with respect to  $x_2/\delta$ , without an indication of the values of  $U_\infty$ ,  $\delta$ , and  $\nu$  or  $R_\delta$ ]. This circumstance also makes it impossible to obtain the dependence  $\epsilon(r)$  from these experimental data.

There are especially few data suitable for analysis of the measurements of the turbulence scale. To obtain the dependence  $\epsilon(r)$ , we must accept some one definition of the turbulence scale for all the experimental data.

In the present work, we have accepted the following definition of the turbulence scale: The scale  $L$  is equal to half the distance  $s$  between points at which the cross correlation function

$$R_{11}(s, x_1, x_2) = \frac{\langle u_1(x_1, x_2 + s/2) u_1(x_1, x_2 - s/2) \rangle}{\sqrt{\langle u_1^2(x_1, x_2 + s/2) \rangle \langle u_1^2(x_1, x_2 - s/2) \rangle}}$$

vanishes with the prescribed accuracy. This meaning of the scale is ascribed to point  $(x_1, x_2)$  lying in the middle of the segment connecting these points. Figure 1 shows a typical shape of the function

$$R_{11}'(s, x_1, x_2) = \frac{\langle u_1(x_1, x_2) u_1(x_1, x_2 + s) \rangle}{\sqrt{\langle u_1^2(x_1, x_2) \rangle \langle u_1^2(x_1, x_2 + s) \rangle}}$$

taken from another paper (Bibl.4). It is evident that  $R_{11}(s)$  and  $R_{11}'(s)$  vanish with the prescribed accuracy at the same values of  $s = 2L$ . The experimental

data (Bibl.4) on measurements of  $R'_{11}(s, x_1, x_2)$  in the boundary layer on a flat plate were analyzed, to obtain the distribution of the scale of turbulence. In

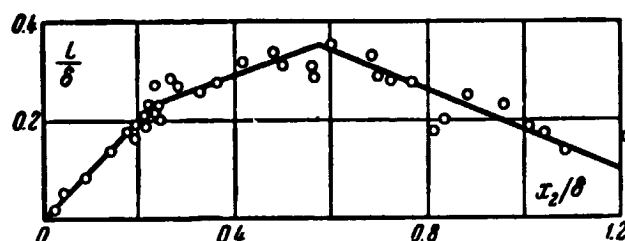


Fig.2

this case, the point to which we must ascribe the value of the turbulence scale, equal to  $L$ , has coordinates  $(x_1, x_2 + L)$  if  $s > 0$ , or  $(x_1, x_2 - L)$  if  $s < 0$ . The results of such an analysis are given in Fig.2. The obtained

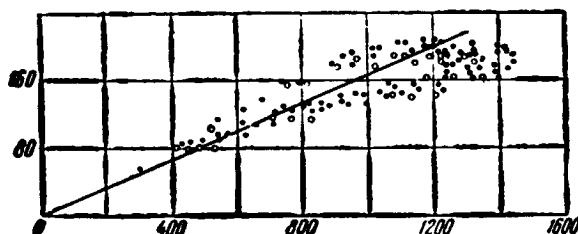


Fig.3

experimental curve was approximated by a broken line. In the present work, it is assumed that the obtained distribution of the turbulence scale holds true at any place of the boundary layer on a flat plate.

The distribution of the quantity  $v_\epsilon/u_{*}\delta$  across the boundary layer of a flat plate, calculated from the data of Klebanov and Townsend, is given in a monograph (Bibl.3). It was found that, in the range of  $3 \times 10^4 < R_\delta < 8 \times 10^4$ ,  $v_\epsilon/u_{*}\delta$  is a function only of  $x_2/\delta$ . The same monograph gives Klebanov's experimental data on the distribution of  $\langle u_1^2 \rangle$ ,  $\langle u_2^2 \rangle$ ,  $\langle u_3^2 \rangle$  across the boundary layer of a flat plate for  $R_\delta = 8 \times 10^4$  ( $u_{*}/U_\infty = 0.037$ ). Using the distribution of

the turbulence scale across the boundary layer shown in Fig.2, we can calculate  $r$  and  $\epsilon$ . The results of this calculation are shown in Fig.3 (black dots).

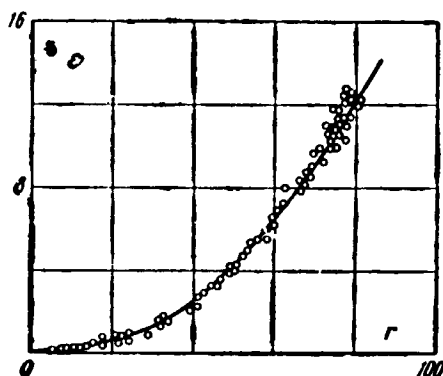


Fig.4

The experimental data on the distribution of  $2e/u_*$  across the boundary layer for  $R_\delta = 7.3 \times 10^4$  are given elsewhere (Bibl.5). These data were also analyzed and are plotted in Fig.3 (points given as circles).

In this range of  $r$  numbers, the dependence  $\epsilon(r)$  was approximated by a linear function:  $\epsilon = \alpha r$ .

The experimental data on the distributions of the components of the turbulent stress tensors, mean velocities, and turbulence scale in the self-similar part of a plane wake behind a cylinder given elsewhere (Bibl.6) were also analyzed to obtain the dependence  $\epsilon(r)$ . The results of this analysis are shown in Fig.4. In this range of  $r$  numbers, the function  $\epsilon(r)$  is satisfactorily approximated by a semicubical parabola:  $\epsilon = \alpha r^2/r_0$ . However, Townsend (Bibl.6) gives data only for the distribution of the integral turbulence scales. We can conclude from these data that the turbulence scale, in the sense of the definition accepted in this work, is constant across the wake and no conclusions can be drawn concerning the magnitude of the scale. Therefore, the scale for  $r$  in Fig.4 is conditional.

4. An analysis of the experimental data on the distribution of the components of the Reynolds stress tensor, the mean velocities, and the turbulence scale made it possible to construct the dependence of "turbulent viscosity" on the Reynolds number of turbulence. This dependence is well approximated by the following piecewise-smooth function

$$e = H(r) \alpha r$$

$$H(r) = \begin{cases} r/r_0 & 0 \leq r/r_0 < 0.75 \\ r/r_0 - (r/r_0 - 0.75)^2 & 0.75 \leq r/r_0 < 1.25 \\ 1 & 1.25 \leq r/r_0 < \infty \end{cases} \quad (4.1)$$

5. Adding of all equations in the system (1.3) will yield the equation /18 for the total turbulent energy:

$$\begin{aligned} & \frac{\partial e}{\partial t} + \sum_{k=1}^3 U_k \frac{\partial e}{\partial x_k} + \sum_{i,k=1}^3 \langle u_i u_k \rangle \frac{\partial U_i}{\partial x_k} + \\ & + \sum_{k=1}^3 \frac{\partial}{\partial x_k} \left[ -\nu \frac{\partial e}{\partial x_k} + \left\langle u_k \cdot \sum_{j=1}^3 \left( \delta_{jk} \frac{1}{\rho} p + \frac{u_j^2}{2} \right) \right\rangle \right] + \nu \sum_{i,k=1}^3 \left\langle \left( \frac{\partial u_i}{\partial x_k} \right)^2 \right\rangle = 0. \end{aligned} \quad (5.1)$$

As a consequence of the continuity equation for velocity fluctuations, we have

$$\frac{1}{\rho} \sum_{i=1}^3 \left\langle p \frac{\partial u_i}{\partial x_i} \right\rangle = 0.$$

If, in eq.(5.1), we make estimates of the terms and discard small terms beginning with the order of smallness  $(\delta/l)^{1/2}$ , we obtain the following equation:

$$-\langle u_1 u_2 \rangle \frac{\partial U_1}{\partial x_2} + \nu \sum_{j,k=1}^3 \left\langle \left( \frac{\partial u_i}{\partial x_k} \right)^2 \right\rangle = 0. \quad (5.2)$$

If, in eq.(5.2), we add a term expressing the diffusion of turbulent energy in the direction  $x_2$  and having an order of smallness of  $(\delta/l)^{1/2}$ , as well as convective terms having an order of smallness of  $(\delta/l)$ , then we obtain an equation analogous to the equation of heat transfer in a compressible laminar boundary layer:

$$U_1 \frac{\partial \sigma}{\partial x_1} + U_2 \frac{\partial \sigma}{\partial x_2} = \frac{\partial}{\partial x_3} \left[ \nu \frac{\partial \sigma}{\partial x_3} - \left\langle u_2 \left( \frac{1}{\rho} p + \frac{u_1^2 + u_2^2 + u_3^2}{2} \right) \right\rangle \right] - \\ - \langle u_1 u_2 \rangle \frac{\partial U_1}{\partial x_2} - \nu \sum_{i,k=1}^3 \left\langle \left( \frac{\partial u_i}{\partial x_k} \right)^2 \right\rangle . \quad (5.3)$$

The addition of these terms will not change the result, since the added terms are small in comparison with the principal terms. As a result, we obtain a system of equations for which methods of numerical integration have been worked out [see, for example, (Bibl.7)].

In eq.(5.3), the term expressing the work of the Reynolds stresses is replaced by its expression in terms of "turbulent viscosity"

$$- \langle u_1 u_2 \rangle \frac{\partial U_1}{\partial x_2} = \nu \epsilon(r) \left( \frac{\partial U_1}{\partial x_2} \right)^2 . \quad (5.4)$$

For the term expressing the dissipation of turbulent energy, we can obtain the following expression, after summing eq.(2.2) with respect to all  $i = j$

$$\nu \sum_{i,k=1}^3 \left\langle \left( \frac{\partial u_i}{\partial x_k} \right)^2 \right\rangle = \nu C (1 + \kappa r) \frac{\epsilon}{L^3} . \quad (5.5)$$

As already indicated above, eq.(2.2) was obtained under rather gross assumptions. It is known from experimental data (Bibl.8) that the energy dissipation at homogeneous turbulence and at large Reynolds numbers is expressed by the formula:

$$\nu \sum_{i,k=1}^3 \left\langle \left( \frac{\partial u_i}{\partial x_k} \right)^2 \right\rangle \approx A \frac{\epsilon^{3/4}}{L} = \nu A r \frac{\epsilon}{L^3} \quad (A = \text{const}) . \quad (5.6)$$

It is also known that at small Reynolds numbers the expression for the turbulent energy dissipation deviates from this law; the character of this deviation has been little studied. We can assume that, at inhomogeneous turbulence as it occurs in the boundary layer, the expression for the turbulent 19 energy dissipation can be written in the following manner:

$$\nu \sum_{i,k=1}^3 \left\langle \left( \frac{\partial u_i}{\partial x_k} \right)^2 \right\rangle = \nu C D(r) \frac{\epsilon}{L^3} \quad (5.7)$$

where  $D(r)$  is a certain function which, when  $r \rightarrow \infty$ , asymptotically approaches a certain straight line passing through the origin of the coordinates. It follows from the experimental data on the attenuation of turbulence at the final period of degeneration (Bibl.8) that for  $r \rightarrow 0$

$$\sum_{i,k=1}^3 \left\langle \left( \frac{\partial u_i}{\partial x_k} \right)^2 \right\rangle \approx \frac{\epsilon}{L^3}.$$

Hence it follows that  $D(r) \rightarrow 1$  when  $r \rightarrow 0$ . However, the character of the behavior of  $D(r)$  for intermediate values of  $r$  has not been studied. Furthermore, caution is recommended in transferring the results of experiments at homogeneous turbulence to turbulent flows with a mean velocity gradient. Unfortunately, to our knowledge there are no experimental data available, from which  $D(r)$  could be determined for the case of turbulent flows with a mean velocity gradient. Therefore, we assume here that

$$D(r) = 1 + \epsilon (\kappa r) \quad (5.8)$$

where  $\kappa$  is a certain constant factor.

The quantity  $D$  can be treated as some "intravortex" "turbulent viscosity" caused by small-scale fluctuations. This interpretation permits the assumption that the term expressing diffusion of the turbulent energy can be expressed in the following manner:

$$\frac{\partial}{\partial x_2} \left[ \nu \frac{\partial \epsilon}{\partial x_2} - \left\langle u_2 \left( \frac{1}{\rho} p + \frac{u_1^2 + u_2^2 + u_3^2}{2} \right) \right\rangle \right] = \frac{\partial}{\partial x_2} \left( \nu D(r) \frac{\partial \epsilon}{\partial x_2} \right). \quad (5.9)$$

Thus, the following system of differential equations is obtained for the turbulent boundary layer:

$$U_1 \frac{\partial U_1}{\partial x_1} + U_2 \frac{\partial U_1}{\partial x_2} = -\frac{1}{\rho} \frac{\partial P}{\partial x_1} + \frac{\partial}{\partial x_2} \left( \nu M \frac{\partial U_1}{\partial x_2} \right); \quad \frac{\partial U_1}{\partial x_1} + \frac{\partial U_2}{\partial x_2} = 0; \quad (5.10)$$

$$U_1 \frac{\partial e}{\partial x_1} + U_2 \frac{\partial e}{\partial x_2} = \frac{\partial}{\partial x_2} \left( \nu D \frac{\partial e}{\partial x_2} \right) + \nu (M-1) \left( \frac{\partial U_1}{\partial x_2} \right)^2 - \nu CD \frac{e}{L^3}.$$

The system (5.10) is closed by the functions

$$M = 1 + \varepsilon(r), \quad D = 1 + \varepsilon(\kappa r), \quad L/\delta = \varphi(x_2/\delta). \quad (5.11)$$

Here  $\varphi(x_2/\delta)$  and  $\varepsilon(r)$  are the empirical functions obtained above in Sections 3 and 4, where the function  $\varphi(x_2/\delta)$ , generally speaking, is valid only for the case of a boundary layer on a flat plate.

6. For the case of a flat plate, the system of equations (5.10), (5.11) was integrated by the net-point method analogous to that described elsewhere (Bibl.7). The boundary conditions for  $x_2 = 0$  were the usual conditions of attachment  $U_1 = U_2 = e = 0$ . For  $x_2 \rightarrow \infty$ ,  $U_1 \rightarrow U_\infty$ , we have  $e \rightarrow 0$ . The integration was started from a certain point of the flat plate, corresponding to a Reynolds number of the order of  $10^4$  plotted for the distance from the leading edge of the plate. Here, it was assumed that the boundary layer was still laminar. Therefore, as the initial mean velocity profile  $U_1(x_{10}, x_2)$  we took the Blasius profile. It was assumed that, in the initial cross section of /20 the boundary layer, small disturbances were present whose energy was distributed across the layer according to the following law:

$$e(x_2) = [\psi(x_2)]^2, \quad \psi(x_2) = \sqrt{e_m} (x_2/x_{2m}) \exp \{1/2 [1 - (x_2/x_m)^2]\}.$$

The function  $\psi(x_2)$  for  $x_2 = x_{2m}$  has a maximum, moreover  $\psi(x_{2m}) = \sqrt{e_m}$ . Here, the obtained distribution of the turbulence energy in the initial cross section satisfies the boundary conditions.

By means of the continuity equation, the first equation of the system (5.10) is transformed into

$$U_1 \frac{\partial U_1}{\partial x_1} - \frac{\partial U_1}{\partial x_2} \int_0^{x_2} \frac{\partial U_1}{\partial x_1} dx_2 = \frac{\partial}{\partial x_2} \left( \nu M \frac{\partial U_1}{\partial x_2} \right). \quad (6.1)$$



The field of integration is covered by a uniform net with intervals of  $\Delta x_1 = h_1$  and  $\Delta x_2 = h_2$ . The partial derivatives in eq.(6.1) are replaced by the finite difference expressions

$$\begin{aligned}\frac{\partial U_1}{\partial x_1} &\approx \frac{1}{h_1} (u_n^{m+1} - u_n^m), \quad U_1 \approx \frac{1}{2} (u_n^{m+1} + u_n^m) \\ \frac{\partial U_1}{\partial x_2} &\approx \frac{1}{2h_2} [\theta (u_{n+1}^{m+1} - u_{n-1}^{m+1}) + (1-\theta) (u_{n+1}^m - u_{n-1}^m)] \\ \frac{\partial}{\partial x_2} \left( M \frac{\partial U_1}{\partial x_2} \right) &\approx \frac{\theta}{h_2^2} [M_{n+1/2}^{m+1/2} (u_{n+1}^{m+1} - u_n^{m+1}) - M_{n-1/2}^{m+1/2} (u_n^{m+1} - u_{n-1}^{m+1})] + \\ &\quad + \frac{1-\theta}{h_2^2} [M_{n+1/2}^{m+1/2} (u_{n+1}^m - u_n^m) - M_{n-1/2}^{m+1/2} (u_n^m - u_{n-1}^m)] \\ M_{n+1/2}^{m+1/2} &\approx \frac{1}{2} (M_{n+1}^{m+1/2} + M_n^{m+1/2}), \quad M_{n-1/2}^{m+1/2} \approx \frac{1}{2} (M_n^{m+1/2} + M_{n-1}^{m+1/2}) \\ u_n^m &= U_1(mh_1, nh_2), \quad M_n^{m+1/2} = M[(m + \frac{1}{2})h_1, nh_2], \quad 0 \leq \theta \leq 1.\end{aligned}$$

The integral in eq.(6.1) is replaced by the expression from the formula for a trapezoid:

$$\int_0^{x_2} \frac{\partial U_1}{\partial x_1} dx_2 \approx \frac{h_2}{2} \left[ \frac{u_n^{m+1} - u_n^m}{h_1} + 2 \sum_{k=1}^{n-1} \frac{u_k^{m+1} - u_k^m}{h_1} + \frac{u_0^{m+1} - u_0^m}{h_1} \right].$$

These relationships approximate the terms entering into eq.(6.1) at the point  $x_1 = (m + \frac{1}{2})h_1$ ,  $x_2 = nh_2$  with an accuracy of  $O(h_2^2) + O(h_1)$ . If we substitute these expressions into eq.(6.1), we obtain the following equation:

$$-\alpha_n u_{n+1}^{m+1} + \beta_n u_n^{m+1} - \gamma_n u_{n-1}^{m+1} - \sigma_n \sum_{k=1}^n u_k^{m+1} = \delta_n. \quad (6.2)$$

Here,  $\alpha_n, \beta_n, \gamma_n, \sigma_n, \delta_n$  are expressed in terms of

$$u_k^m \quad (k = 1, 2, \dots, n+1), \quad u_s^{m+1}, \quad M_s^{m+1/2} \quad (s = n-1, n, n+1)$$

and also  $M_s^{m+1/2} = M(r_s^{m+1/2})$ , where

$$\begin{aligned}r_s^{m+1/2} &= v^{-1} \sqrt{(e_s^{m+1} + e_s^m)/2} \delta_{m+1/2} \varphi(sh_2/\delta_{m+1/2}) \\ \delta_{m+1/2} &= 0.5 [\delta((m+1)h_1) + \delta(mh_1)].\end{aligned}$$

In the same manner, we can obtain the difference equation approximating with the same accuracy the differential equation of the energy of turbulence at the point  $(x_1 = (m + \frac{1}{2})h_1, x_2 = nh_2)$

$$-\alpha_n' e_{n+1}^{m+1} + 3\alpha_n' e_n^{m+1} - \gamma_n' e_{n-1}^{m+1} = \delta_n' . \quad (6.3)$$

In the expression for the coefficients of eqs.(6.2) and (6.3), the quantities  $u_{n+1}^{m+1}$ ,  $u_n^{m+1}$ ,  $u_{n-1}^{m+1}$ ,  $e_{n+1}^{m+1}$ ,  $e_n^{m+1}$ , and  $e_{n-1}^{m+1}$  enter as sums of the type  $(u_k^{m+1} + u_k^m)$ ; therefore, for small intervals of  $h_1$  the values of these sums and thus also the coefficients of eqs.(6.2) and (6.3) change little if we replace  $u_k^{m+1}$ ,  $e_k^{m+1}$  by  $u_k^m$ ,  $e_k^m$ . This permits calculating the coefficients of eqs.(6.2) in first approximation, assuming that  $u_k^{m+1} = u_k^m$ . In this case, we obtain a system of 21 linear algebraic equations which is solved by the method of successive elimination of unknowns, using the boundary condition  $u_0^{m+1} = 0$ . Here, the system of equations (6.1), for various  $n = 1, 2, \dots, N$ , reduces to the form

$$u_n^{m+1} = A_n u_{n+1}^{m+1} + B_n \quad (n = 1, 2, \dots, N) . \quad (6.4)$$

The edge of the boundary layer is found from two conditions:

$$U_1|_{x_1=\delta} = U_\infty, \quad (\partial U_1 / \partial x_2)|_{x_1=\delta} = 0 . \quad (6.5)$$

Condition (6.5) with consideration of eq.(6.4) was transformed into

$$u_{N+1}^{m+1} = U_\infty, \quad U_\infty (1 - A_N) - B_N < \varepsilon_1 . \quad (6.6)$$

From the last condition in the system (6.6), we determined the number of the point  $N$  at which  $\partial U_1 / \partial x_2$  vanishes with the prescribed accuracy. We then

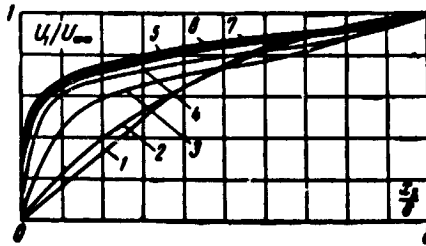


Fig.5

determined all  $u_n^{m+1}$  in sequence, after which the values of  $e_n^{m+1}$  were determined in the same manner. In this case, the values of  $u_k^{m+1}$  obtained in the first

approximation were substituted into the formulas of the coefficients of eqs.(6.3).

The calculation was then repeated for  $u_k^{n+1}$ ,  $e_k^{n+1}$  of the first approximation to find the values of  $u_k^{n+1}$ ,  $e_k^{n+1}$  of the second approximation, and so forth. The process of iteration continued until the thickness of the momentum loss

$$\delta_{**} = \int_0^{\infty} \frac{U_1}{U} \left(1 - \frac{U_1}{U_{\infty}}\right) dx_2$$

stopped changing from iteration to iteration with a certain accuracy  $\epsilon_2$ .

The boundary-layer thickness in each iteration, needed for the calculation of  $r$ , was determined from the condition  $U_1 = 0.99 U_{\infty}$  since the distribution of the scale across the boundary layer shown in Fig.2 was obtained precisely with such a determination of the boundary-layer thickness.

Thus, having determined the distribution of the velocity  $U_1$  and of the turbulent energy for a certain  $x_1 = m_0 h_1$ , we can calculate the distribution  $U_1$  ( $[m_0 + 1] h_1, kh_2$ ),  $e$  ( $[m_0 + 1] h_1, kh_2$ ), and so forth. The number of points  $N$  across the layer increases with an increase in boundary-layer thickness. At the end of the calculation for  $x_1$  corresponding to a Reynolds number of  $R \approx 3.5 \times 10^6$ , we have  $N \approx 700$ .

Before integrating the system of equations (5.10), (5.11), the boundary and initial conditions were reduced to a dimensionless form. The quantities  $\epsilon_1$  and  $\epsilon_2$  were equal respectively to  $10^{-3}$  and  $10^{-6}$ . To find the friction coefficient of the plate  $C_f$ , we used the integral relation integrated along the plate. The momentum loss thickness entering into this relation was determined from the resultant distribution  $U_1$ . The value of  $\partial U_1 / \partial x_2$  for  $x_2 = 0$ , needed for the calculation of  $u_{*}$ , was determined from the values of  $U_1$  at the points  $x_2 = 0, h_2, 2h_2$ . In this case we used the fact that, at  $x_2 = 0$ , we have  $\partial^2 U_1 / \partial x_2^2 = 0$

on the plate.

To define the accuracy of the calculations, certain computations were checked with half-intervals. It was found that the values of  $C$ , in the calculations agreed with an accuracy of 1.5 - 2%.

As mentioned above, as a consequence of the large scattering of the experimental data, the values of the constants  $\alpha$ ,  $r_0$ ,  $C$ ,  $\kappa$  and the function  $\varphi(x_2/\delta)$  could not be determined with sufficient accuracy. Therefore, a series of calculations was checked to select the values of the constants and the function  $\varphi(x_2/\delta)$ . The constants varied within the scattering of the experimental data. For each variant of the values of the constants, we calculated the flow in the boundary layer of a flat plate. The results of the calculation were compared with the experimental data obtained for the velocity profiles, energy of turbulence, and dependence of the coefficient of friction on the Reynolds number. As a result of this series, we selected values of the constants which simultaneously gave satisfactory agreement between the indicated calculated functional dependences and the experimental. The following values of the constants were selected:  $\alpha = 0.2$ ,  $r_0 = 110$ ,  $C = 3.93$ ,  $\kappa = 0.4$ . The function  $\varphi(x_2/\delta)$  is shown in Fig.2 as a broken line.

With the selected values of the constants we carried out a series of 22 calculations of flow in the boundary layer of a flat plate for various values of  $e$ , lying in the range

$$0.0001 < \sqrt{e_m} / U_\infty < 0.1 .$$

Figure 5 shows the mean velocity distributions obtained as a result of integration of the system of equations (5.10), (5.11) for  $\sqrt{e_m}/U_\infty = 0.05$ , and Fig.6 gives the corresponding energetic velocity of turbulence  $\sqrt{e}/U_\infty$ . The numerals 1 and 2 in the diagrams denote the distributions obtained at distances

$x_1$  from the leading edge of the plate corresponding to Reynolds numbers of  $1.25 \times 10^4$  and  $4.82 \times 10^4$ . At these Reynolds numbers, the character of the

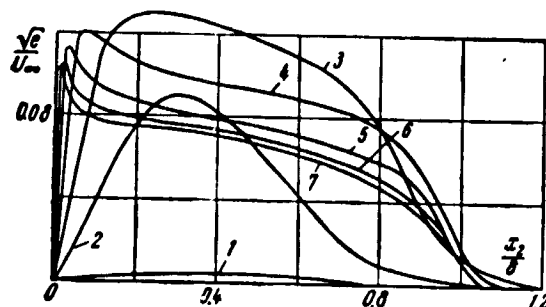


Fig.6

mean velocity distribution is still very close to laminar, and the maximal value of the energetic velocity of turbulence gradually increases. The numerals 3, 4, 5 in the diagrams correspond to Reynolds numbers of  $1.22 \times 10^5$ ,

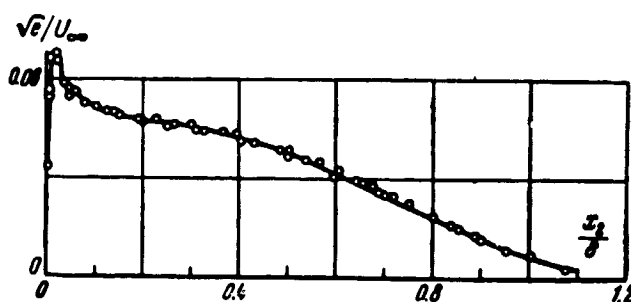


Fig.7

$4.07 \times 10^5$ , and  $9.78 \times 10^5$ . In this region a gradual deviation of the character of the distribution of mean velocity from laminar and an approach to turbulent is noted.

The energetic velocity of turbulence at first increases markedly and then begins to diminish, more rapidly in the outer part of the boundary layer owing to the decrease in the mean velocity gradient in this portion. The distribution of the energetic velocity of turbulence shows a characteristic maximum near the wall which becomes ever sharper. The numerals 6 and 7 correspond to Reynolds

numbers of  $2.12 \times 10^6$  and  $3.51 \times 10^6$ . The distribution of the mean and energetic velocities of turbulence in this range depends weakly on the Reynolds number. For a comparison, Fig.7 shows the distribution of the energetic velocity

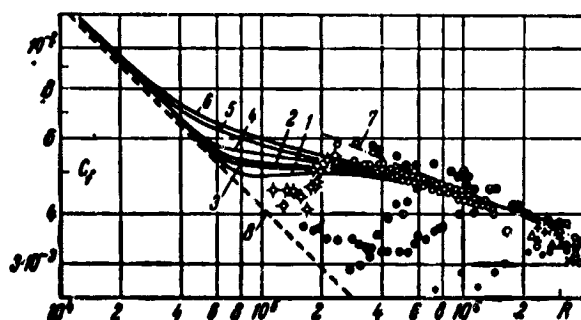


Fig.8

of turbulence at a Reynolds number of  $4.2 \times 10^6$  obtained from an analysis of the experimental data cited elsewhere (Bibl.3). The comparison of Figs.6 and 7 can

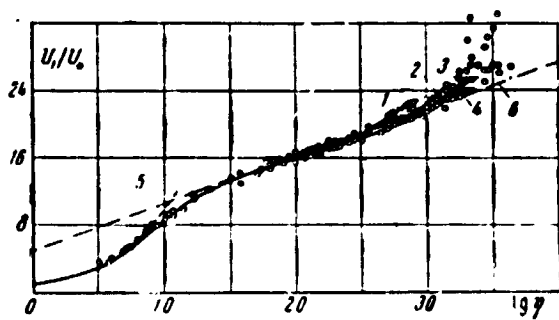


Fig.9

be only qualitative since the last of the curves in Fig.6 was obtained at a Reynolds number of  $3.51 \times 10^6$ . In addition, the system of equations (5.10), (5.11) was integrated at boundary conditions for a turbulent energy  $e \rightarrow 0$  when  $x_2 \rightarrow \infty$ , whereas the experimental distribution of the energetic velocity of turbulence was obtained in the presence of turbulent perturbations in the outer flow.

The laminar, transitional, and turbulent regions of the solution of the system of equations (5.10), (5.11) can be traced more distinctly by examining

the obtained dependences of the friction coefficient  $C_f$  on the Reynolds number  $R = U_\infty x_1/\nu$ , which are shown in Fig.8. The experimental data of various authors, cited in another paper (Bibl.1), are marked by dots in Fig.8. The dashed curve No.8 in Fig.8 corresponds to the dependence on the theory of a laminary boundary layer. The dot-dash curve No.7 corresponds to the experimental dependence  $C_f = 0.455 (\log R)^{-2.58}$  for a turbulent boundary layer. The solid curves Nos.1 - 6 correspond to solutions of the system (5.10), (5.11), obtained at various values of the quantity  $\sqrt{e_n}/U_\infty$  given in the initial cross section. The curves

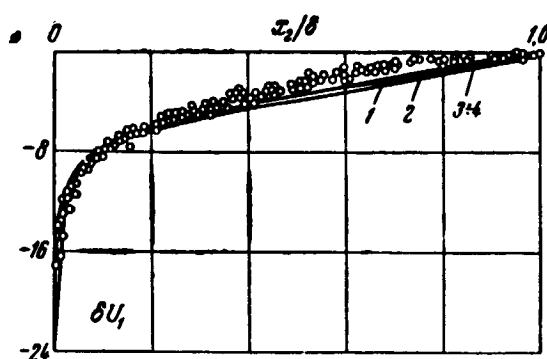


Fig.10

Nos.5 and 6 in Fig.8 correspond to large values of  $\sqrt{e_n}/U_\infty$  in the initial cross section (0.05 and 0.1, respectively). At large values of  $e_n$  in the initial cross section the dependence  $C_f(R)$  rapidly deviates from laminar. However, the end of the transition zone for all values of  $e_n$  remains the same. Curves Nos.1, 2, 3, 4 correspond to small values of  $\sqrt{e_n}/U_\infty$  (0.0001, 0.0005, 0.001, 0.005). At these values of  $e_n$ , the start of the transition zone shifts to the range of large values of  $R$  and the slope of the curve changes somewhat: A minimum appears on the curve  $C_f(R)$ .

At numbers  $R > 4 \times 10^5$  the dependences  $C_f(R)$  for all values of  $e_n$  merge into one, enter the domain of the scattering of the test points, and proceed almost parallel to curve No.7. The distribution of the mean velocity, shown

in Fig.5, still does not give a complete idea as to the conformity of the solutions of the system of equations (5.10), (5.11) with the experimental data in the turbulent region of the solution. Therefore, the curves Nos.5, 6, 7 in Fig.5 and the distribution of the mean velocity obtained for  $R = 3.26 \times 10^6$  are plotted in Fig.9 as a function of  $U_1/u_* = f(\eta)$  ( $\eta = u_* x_2/\nu$ ). The curve No.5 in Fig.9 corresponds to the dependence  $U_1/u_* = \eta$  and the curve No.6 to  $U_1/u_* = 4.9 + 5.6 \log \eta$ . The experimental data of various authors (Bibl.9) are shown as dots in Fig.9. The solid curves Nos.1, 2, 4 correspond to the distributions 5, 6, 7 in Fig.5, while the curve No.3 corresponds to  $R = 3.26 \times 10^6$ . For  $\log \eta < 2.5$ , all distributions of the mean velocity, in these variables, yield one curve which proceeds in the domain of scattering of the test points. The curves stratify in the outer part of the boundary layer, deviating upward, which corresponds to the ideas developed elsewhere (Bibl.9). Figure 10 shows the same mean velocity distribution as in Fig.9, in the form of the dependence  $\delta U_1 = (U_1 - U_\infty)/u_*$  on  $x_2/\delta$ . This dependence characterizes the velocity distribution in the outer part of the boundary layer.

#### BIBLIOGRAPHY

1. Loytsyanskiy, L.G.: Fluid and Gas Mechanics (Mekhanika zhidkosti i gaza). Gostekhteorizdat, 1957.
2. Rotta, I.: Statistical Theory of Nonhomogeneous Turbulence (Statistische Theorie nichthomogener Turbulenz). Z. Physik, Vol.129, No.6, pp.547-572, 1951.
3. Khintse, I.O.: Turbulence (Turbulentnost'). Fizmatgiz, 1963.
4. Zakharov, Yu.G., Respikh, Ye.U., Filippov, V.M., and Vinogradov, M.N.: Investigation of the Basic Characteristics of Turbulence in the Boundary



Layer of a Flat Plate (Issledovaniye osnovnykh kharakteristik turbulentnosti v pogranichnom sloye ploskoy plastiny). Tr. Tsentr. AGI, 1959.

5. Shubauer, G. (Schubauer, H.): Turbulent Process Observed in a Boundary Layer and Tunnel (Russian Translation of "Mekhanika", Collection of Translations and Review of Foreign Periodical Literature [Turbulentnyye protsessy, nablyudayemye v pogranichnom sloye i trube (Russk. perevod "Mekhanika", Sb. perev. i obz. inostr. period. lit.)]. No.3(31), 1955.
6. Townsend, A.A.: Structure of Turbulent Flow with Transverse Shear (Struktura turbulentnogo potoka s poperechnym sdvigom). Izd. Inostr. Lit., 1959.
7. Brailovskaya, I.Yu. and Chudov, L.A.: Solution of the Boundary-Layer Equation by Various Methods. Collection of Works of the Moscow State University Computer Center "Computer Methods and Programing" (Resheniye uravneniya pogranichnogo sloya raznostnym metodom. Sb. rabot Vychisl. tsentra MGU "Vychislitel'nyye metody i programmirovaniye"). Izd. Mosk. Gos. Univ., 1962.
8. Betchelor, Dzh. (Batchelor, J.): Theory of Homogeneous Turbulence (Teoriya odnorodnoy turbulentnosti). Izd. Inostr. Lit., 1955.
9. Klausner (Clauser), F.: Turbulent Boundary Layer. Collection of Articles Edited by H.Dreiden and T.Karman. "Problems of Mechanics" (Turbulentnyy pogranichnyy sloy. Sb. statey pod red. Kh.Draydena i T.Karmana. "Problemy mekhaniki"). Izd. Inostr. Lit., No.2, 1959.

Received April 27, 1964